

Early Miocene European loess: A new record of aridity in southern Europe

Davor Pavelić^{1,†}, Marijan Kovačić², Adriano Banak³, Gonzalo Jiménez-Moreno⁴, Frane Marković², Kristina Pikelj², Alan Vranjković⁵, Lucija Premužak², Darko Tibljaš², and Mirko Belak³

¹Faculty of Mining, Geology and Petroleum Engineering, University of Zagreb, Pierottijeva 6, HR-10000 Zagreb, Croatia

²Faculty of Science, University of Zagreb, Horvatovac 95, HR-10000 Zagreb, Croatia

³Croatian Geological Survey, Sachsova 2, HR-10000 Zagreb, Croatia

⁴Departamento de Estratigrafía y Palaeontología, Universidad de Granada, Fuente Nueva S/N, 18002, Granada, Spain

⁵NIS a.d., Gazprom Neft, Science and Technology Center, Narodnog fronta 12, 21000 Novi Sad, Serbia

ABSTRACT

The intercalation of silty units and coarse-grained units represented by conglomerates and breccia characterizes a Lower Miocene terrestrial sedimentary sequence in the North Croatian Basin, a part of the southwestern Pannonian Basin system. These sediments were previously interpreted as alluvial sediments, where the silty units would reflect deposition on a floodplain. However, in this study, we show new results that support a different interpretation of the genesis of the silty units. The units, which vary in thickness between 6 and 180 cm, are mostly composed of structureless loose silt. They are brownish yellow to yellowish brown in color and do not contain fossils. Scanning electron microscopy indicated that quartz grains show fracture faces, conchoidal fractures, V-shaped percussion marks, linear steps, and conchoidal crushing features. Such microtextures together with the macroscopic characteristics of the silt units indicate that they were deposited by wind. Therefore, this study reports the first occurrence of Miocene loess outside of China. Silt-sized particles were probably produced by salt-weathering processes on salina-type lake flats during long arid periods. Alluvial deposition was controlled by a more humid climate, so the intercalation of eolian silty units with alluvial conglomerates and breccias reflects alternation of arid and more humid periods in the early Miocene. This agrees with regional paleoclimate studies that show cyclicity in the climate, with a dry cycle and orbital-scale climate variability controlling paleoenvironmental and sedimentary changes in the area during the early Miocene.

INTRODUCTION

Eolian dust has been the subject of research for two main reasons: its debatable origin and use for paleoclimate modeling studies (i.e., Guo et al., 2002; Smalley et al., 2011). Usually, deposits of eolian dust have been referred to as loess (von Leonhard, 1823–1824). There are several definitions of loess, and the simplest one defines it as clastic sediments composed predominantly of silt-sized particles, which are formed by the accumulation of windblown dust (Pye, 1995). Loess usually contains some percentage of sand and clay, in addition to the silt-sized particles. There are three fundamental requirements necessary for loess formation: a sustained dust source, adequate wind energy to transport the dust, and a suitable accumulation area (Pye, 1995; Smalley, 1995; Muhs, 2007; Smalley et al., 2011). There are several different main mechanisms that may produce silt-sized particles, including the release of preexisting silt-sized particles from parent rocks, glacial grinding, frost weathering, fluvial abrasion and crushing, eolian abrasion, salt weathering, chemical weathering, clay pellet aggregation, and biological processes (Pye, 1995).

Loess is frequently associated with soil horizons that indicate alternation of cold and dry periods with warmer and wetter periods, comprising sequences up to a few hundred meters in thickness. As a result loess/paleosol sequences are particularly important in Earth history because they may provide a detailed record of climatic and environmental changes (e.g., Kukla, 1987; Pye, 1995; Smalley, 1995).

Loess deposits are widespread over the world and are mostly of Pleistocene age, when glacial grinding produced a large amount of silt-sized particles and aridity characterized the global climate (Muhs, 2013, and references therein). Holocene loess has been found in many regions too, including deserts, where several silt-producing mechanisms can occur (Smith et al.,

2002; Smalley et al., 2011). Miocene eolian dust deposits have only been reported in China, where the deposit forming loess, and red beds composed of ultrafine eolian dust, was initiated ca. 29 Ma and continued until the Quaternary (e.g., Guo et al., 2002; Liu et al., 2003; Garzzone et al., 2005; Sun et al., 2010; Zhan et al., 2010; Qiang et al., 2011; Stevens et al., 2013a; Nie et al., 2014), although some of the sedimentary sequences are the subject of a debate about their eolian origin (Alonso-Zarza et al., 2009; Guo et al., 2010). Pleistocene loess deposits are well known in southern Central Europe, covering large areas, as well as in Croatia (Haase et al., 2007; Galović et al., 2009; Wacha et al., 2011; Banak et al., 2012, 2013). Recently, Pliocene red clays from Hungary have been interpreted as having an eolian origin (Kovács, 2008; Kovács et al., 2011).

Here, we studied a terrestrial sedimentary sequence in the southwestern Pannonian Basin system in southern Central Europe that indicates eolian dust accumulation in the late early Miocene and thus the existence of the oldest known European loess. Quartz silt-sized particles were probably produced by salt-weathering processes on a salina-type lake flat, and the particles were then deflated and redeposited in the Mount Požeška area. The observed intercalations of the loess units with alluvial coarse-grained deposits suggest alternation of arid and more humid periods under a relatively warm period. This study supports the late early Miocene as a time of relative global warming, which culminated in the Miocene climatic optimum (sensu Zachos et al., 2001), mediated by orbital-scale climate variability (i.e., Jiménez-Moreno et al., 2005, 2008, 2009).

GEOLOGICAL SETTING

The North Croatian Basin is a southwestern satellite basin of the Pannonian Basin system, the formation of which commenced in the early

[†]dpavelic@rgn.hr

SEDIMENTOLOGY AND STRATIGRAPHY OF THE SYNRIFT DEPOSITS

The oldest deposits occurring in the area are of freshwater origin and do not include biostratigraphically valid fossils, so their stratigraphic interpretation was based on superposition and the continuity of sedimentation from alluvial-fan to marine environments (Fig. 4). Deposition probably commenced in the late early Miocene and was mostly characterized by alluvial coarse-grained sediments laid down during the formation of half grabens in the early stage of the synrift phase in the North Croatian Basin (Pavelić, 2001; Malvić, 2012). Pyroclastics, represented by clayey biotite-bearing ash, intercalated with alluvial deposits yielded a $^{40}\text{Ar}/^{39}\text{Ar}$ age of 18.07 ± 0.07 Ma at the northwestern margin of the basin, indicating a middle Burdigalian age (Pavelić et al., 2001; Mandić et al., 2012). The late early Miocene deposits are best developed on Mount Požeška, where elevated footwalls were intensely eroded, and the main depocenters were located in braided alluvial fans (Fig. 3; Pavelić and Kovačić, 1999). Sedimentation was dominated by coarse-grained over fine-grained deposits, with conspicuous variations in grain size but lacking in a sandy fraction in the oldest section, rapid lateral and vertical facies alternations, rare occurrences of red beds and laminated calcretes as pedogenically formed carbonates, and a lack of fauna (i.e., molluscs and micromammals). Coarse-grained deposits are characterized by rock-fall breccias as a consequence of periodic tectonic block uplifting and talus forming over the alluvial-fan deposits, and midfan channel and longitudinal bar conglomerates. The petrographic composition of the coarse-grained material is mostly represented by low-grade schists, while some siliciclastic and magmatic rocks occur rarely. These deposits are intercalated with structureless silty units that may have thin conglomerate lenses. The fine-grained units were previously interpreted as floodplain deposits in the context of the alluvial-fan environment (Pavelić and Kovačić, 1999). Paleocurrent measurements indicated paleotransport of the alluvial material toward the N and NE, where a penecontemporaneous salina-type lake existed (Fig. 3). The lake sedimentation was characterized by the predominance of siliciclastics that formed pelite layers over dolomites, tuffs, and tuffites with analcime. Tuffitic sediments contain minerals of pyroclastic (quartz, feldspars, biotite, volcanic glass) and terrigenous (quartz, muscovite, chlorite, feldspars, lithic fragments) origin, while garnets and amphiboles are the most abundant heavy minerals (Šćavničar et al., 1983). Some

Miocene due to continental collision and subduction of the European plate beneath the African (Apulian) plate (Fig. 1). The first phase of basin development was characterized by tectonic thinning of the crust and isostatic subsidence (synrift), while the second phase was marked by cessation of rifting and subsidence caused by cooling of the lithosphere (postrift; Royden, 1988). The Pannonian Basin system is surrounded by the Alps, Carpathians, and Dinarides, and paleogeographically, it belongs to the Central Paratethys realm (Fig. 2; Harzhauser and Piller, 2007).

The North Croatian Basin covers almost the entire area of north Croatia. It is characterized by WNW-ESE-trending elongated and tectonically subsided zones of depressions with a maximum depth of pre-Miocene substrata of ~6500 m (Fig. 1). On the basis of the depositional history during the early Miocene, it was concluded that the basin was generated by continental passive rifting (Pavelić, 2001). In the central part of the basin, these depressions are bounded by mountains uplifted during the Pliocene and Quaternary, producing a new tectonic pattern in the North Croatian Basin (Márton et al., 1999, 2006). They include Mount Papuk, Mount Krndija, Mount Psunj, Mount Požeška, and Mount Dilj, which are jointly referred to as the Slavonian Mountains.

The Miocene deposits on the Slavonian Mountains unconformably overlie strongly tectonized basement, which is mostly composed of various metamorphic and magmatic rocks generated by the Variscan orogeny and Cretaceous collisional-extensional processes, such as greenschist- and amphibolite-facies metamorphic rocks associated with penecontemporaneous migmatites and granites. These rocks are associated with Silurian to Mississippian low-grade metapelites and metapsammites intruded by metabasic sills. Mesozoic formations are subordinate and are represented by Triassic, Jurassic, and Upper Cretaceous siliciclastic and carbonate rocks, and by Upper Cretaceous igneous and sedimentary rocks (Fig. 3).

The early and middle Miocene synrift fill in the area of the Slavonian Mountains is characterized by deposition in different environments and the occurrence of volcanic activity. The environments changed from terrestrial to marine and were strongly controlled by tectonics, climate change, and eustatic sea-level fluctuations representing a generally long-term transgressive cycle. Three synrift formations can be distinguished: (1) late Burdigalian alluvial and salina-type siliciclastic deposits, (2) early Langhian lacustrine siliciclastics and pyroclastics, and (3) Langhian to Serravallian marine clastics, carbonates, volcanics, and pyroclastics, which are characteristic of the entire North Croatian Basin (Pavelić, 2001; Čorić et al., 2009).

fragments of terrestrial plants, small coal fragments, and molluscs occur within the deposits. Lake deposition reflects the alternation of arid intervals that resulted in high salinity with more humid intervals characterized by lower salinity (Šćavničar et al., 1983). Sedimentology of the alluvial and lacustrine deposits indicates that the early Miocene climate was characterized by cyclicality, alternating between arid and more humid intervals (Šćavničar et al., 1983; Pavelić and Kovačić, 1999). After the end of the alluvial phase in the late Burdigalian, a hydrologically open lake formed, covering a large area in the beginning of the Serravallian. Sedimentation was primarily characterized by fine-grained deposits with an abundance of terrestrial plant fragments (Pavelić, 2001). The forest dwellers *Prodeinotherium bavaricum* (Proboscidea, Mammalia) were found in lacustrine deposits of the nearby Mount Moslavačka, indicating a humid climate and an age between the latest Burdigalian and the early Serravallian (Fig. 4; Krizmanić, 1995). A rich paleofloristic assemblage represented by the remains of leaves indicated a subtropical climate with variable precipitation that controlled lake development (Jamičić et al., 1987; Jungwirth and Đerek, 2000). Sediments containing calcareous nannoplankton belonging to the NN5 zone suggest that the lacustrine phase ended with a short-lived brackish-water interval and culminated with full marine flooding in the Langhian (Pavelić et al., 1998; Čorić et al., 2009; Hajek-Tadesse et al., 2009; Fig. 4).

METHODS

In this study, we focused on the sediments belonging to the late Burdigalian alluvial units from the northern slopes of Mount Požeška, where gravels, breccia, and silts are intercalated. The goal is a reexamination (from the eolian depositional point of view) of silts that were previously interpreted as resulting from floodplain deposition. The difference between floodplain and eolian deposition can be indicated by a detailed study of the silt in the field, the grain size of the silt, provenance analysis, microtextures of silt quartz grains, and palynological analysis. A comparison with Croatian Pleistocene loess grain size from BANSKO HILL can additionally help the interpretation of the genesis of the late Burdigalian silt on Mount Požeška (Fig. 1).

Field Study

In order to interpret the depositional mechanism of the silt from Mount Požeška, we carried out a field study that included measure-

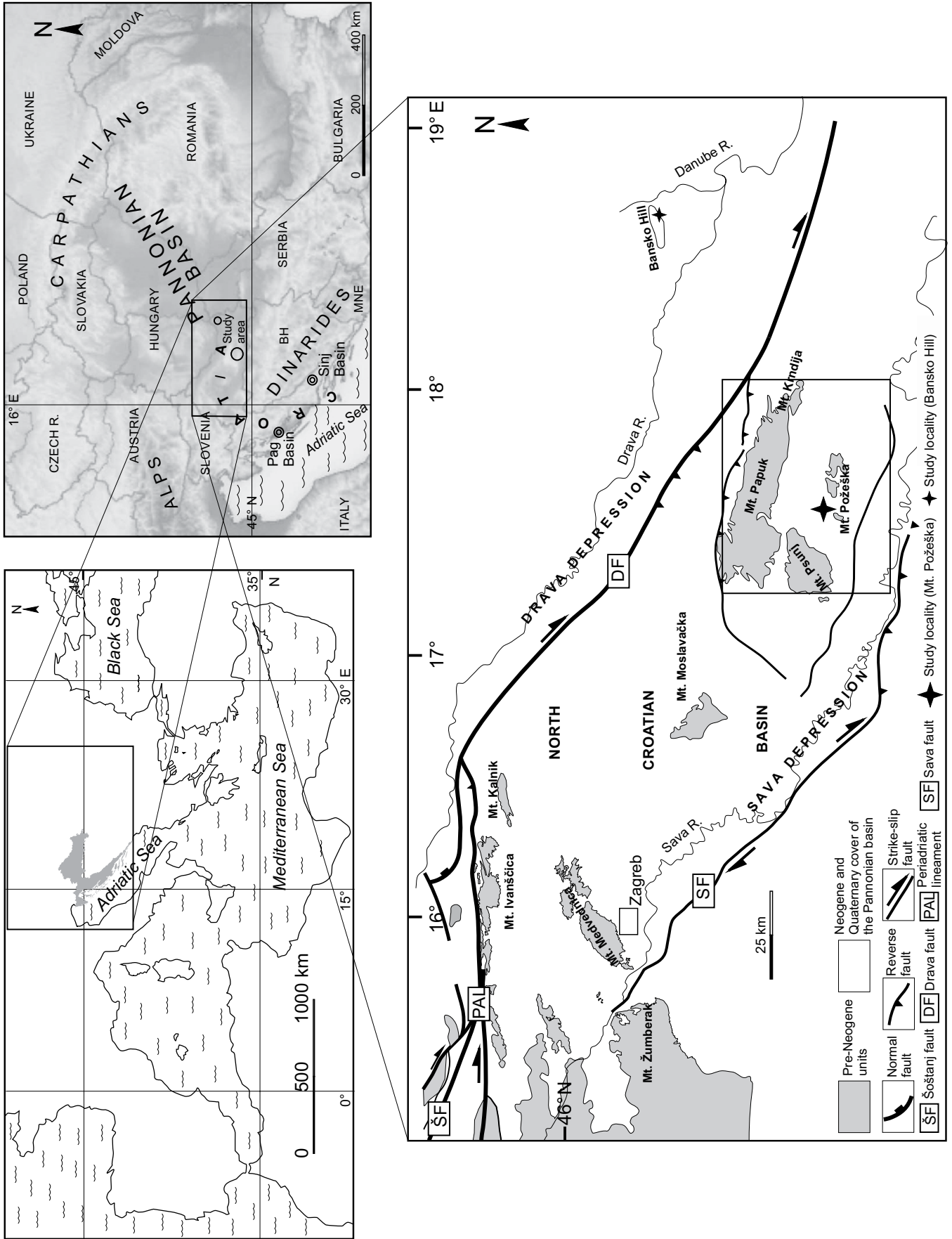


Figure 1. Location map. The study area is located on Mount Požeška (large asterisks), which belongs to the North Croatian Basin as a part of the southwestern Pannonian Basin system. The location of the studied Pleistocene loess on the Banskó Hill (small asterisk) is also indicated. Main faults are modified after Márton et al. (2002).

Figure 2. Paleogeographic sketch map of the circum-Mediterranean area with focus on the Paratethys Seas in the early Miocene (Harzhauser and Piller, 2007). The asterisk shows the tentative position of Mount Požeška.



ments of the thickness of fine-grained units, the character of their bedding planes and internal structures, and fossil investigations. Color was determined using the Munsell Color Chart (Goddard et al., 1963). Several samples of fine-grained deposits were selected for more detailed analyses. Five samples were taken from the Pleistocene loess on BANSKO HILL in Baranja, eastern Croatia (Zmajevac locality), for comparison.

Grain-Size Analysis

In total, 23 bulk samples were taken from the late Burdigalian silts from Mount Požeška, and five samples were taken from the Pleistocene loess from BANSKO HILL for grain-size analysis and comparison (Figs. 5A and 5B). The samples

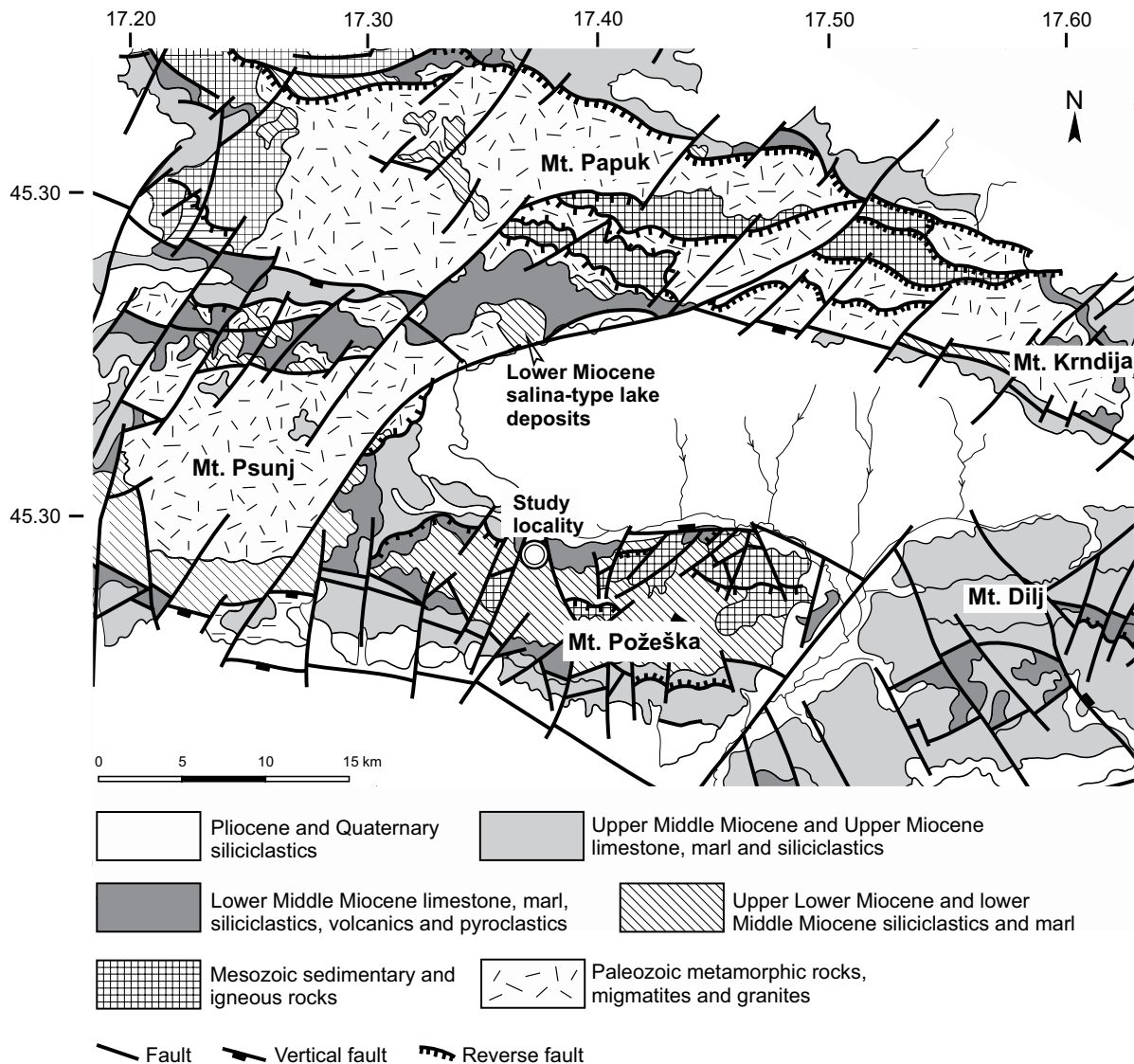


Figure 3. A simplified geological map of the Slavonian Mountains area (after HGI, 2009).

were air-dried prior to grain-size analysis. Approximately 100 g aliquots of each sample were separated, weighed, and disaggregated in distilled water. Samples were then wet-sieved through a set of seven sieves (4 mm to 32 μm) at an interval of one phi. Wet mud containing particles <32 μm was disaggregated in sodium metaphosphate solution using an ultrasonic bath and subsequently analyzed using SediGraph (model 5100). The particle size range employed for SediGraph analysis was 0.5–63 μm , in order to overlap data obtained by both techniques. Distributions of both measurements were renormalized and merged. The grain-size statistics were calculated using Gradistat software (Blott and Pye, 2001).

Modal Analysis

The modal compositions of six samples from the late Burdigalian silts from Mount Požeška were analyzed to determine the composition and provenance of the material. The analysis was performed on the 0.063–0.125 mm fraction. Heavy and light mineral fractions (HMF and LMF) were separated by bromoform liquid (CHBr_3 ; $\delta = 2.86 \text{ g cm}^{-3}$). Qualitative and quantitative analyses of HMF and LMF were performed by identifying 300–350 grains per sample under a polarization microscope (following the method of Mange and Maurer, 1992).

Scanning Electron Microscopy (SEM)

Ten samples were taken from the silty units from Mount Požeška and examined using a scanning electron microscope (PG-3, PG-6, PG-9, PG-11, PG-13, PG-16, PG-20, PG-21, PG-22, and PG-23; Fig. 5A). Finally, four samples were chosen for analysis after light mineral fraction extraction (PG-20, PG-21, PG-22, and PG-23). We focused on quartz grains, analyzing their shape and the detailed morphology of the grain surface. Grains in samples were coarse silt-sized (40–63 μm) and sand-sized particles (>63 μm). The samples were glued to a carrier with double-sided tape and then steamed with gold having a thickness of 15 nm. Prepared samples were placed in a container and analyzed using a scanning electron microscope JEOL, model JSM-6510 LV, within a magnification range of 450 \times –5000 \times , in the Laboratory of Geochemistry, INA-Industrija Naft, d.d., Zagreb. More than 70 different grains were imaged, and the best photographs showing complete quartz grains were selected. The quartz grain surface microtexture classification method and terminology are based on studies by Mahaney and Andres (1996), Van Hoesen and Orndorff (2004), and Vos et al. (2014).

Palynological Analysis

Nine samples were taken from the fine-grained facies from Mount Požeška (PG-1, 3, 4, 5, 16, 18, 20, 21, and 22; Fig. 5A). They were processed following the standard protocol used by Faegri and Iversen (1989), with HF and HCl for mineral digestion, sieving through 250 and 10 μm sieves, and addition of Zn_2Cl for density separation. The remaining residue was mounted together in glycerin on glass slides. Slides were examined using a transmitted light microscope at 200 \times and 400 \times magnifications.

RESULTS

Field Description of Fine-Grained Deposits

In this study, we analyzed fine-grained deposits that alternate with coarse-grained siliciclastics in a 109-m-thick section located on the northern slopes of Mount Požeška (Fig. 1). The fine-grained units are represented by loose silt varying in thickness between 6 and 180 cm (Figs. 5A and 6). The cumulative thickness of the silt units is ~25.5 m. The lower boundary of the units is irregular, while the upper boundaries usually indicate strong erosion. The units lack any type of internal structures (Fig. 6C). They are either brownish yellow (10YR 6/8) or yellowish brown (10YR 5/6) in color, sometimes with bluish gray mottling (GLEYS 5/5B; Figs. 6A and 6B). Red coloration (10R 4/4) or laminated calcretes that are a few centimeters thick occur on the upper part of some of the sedimentary units, which probably indicate postdepositional processes (Fig. 6C). Thin conglomerate lenses or isolated grains up to 5 mm in diameter occur within some thicker units (Fig. 6D).

Grain-Size Analysis

Grain-size analysis of sediments from Mount Požeška indicates silt as the dominant grain-size fraction in 21 of the 23 studied samples (Fig. 5A; Table 1). Clay is prevalent in the remaining two samples (PG-3 and PG-4). The abundance of the silt-sized fraction in all samples ranges from 33% to 80%, and the average value is 57.70%. Besides the silt-sized particles, the samples contain 3%–58% clay-sized particles, 4%–38% sand-sized particles, and <4% gravel-sized particles (Table 1). The average percentage for clay-sized particles is 23.73%, sand-sized particles is 18.08%, and gravel-sized particles is only 0.5%. Median grain size (Md) in 20 samples varies in the range of very fine to medium silt (4–32 μm). The exceptions are clay-rich samples PG-3 and PG-4, with a median size

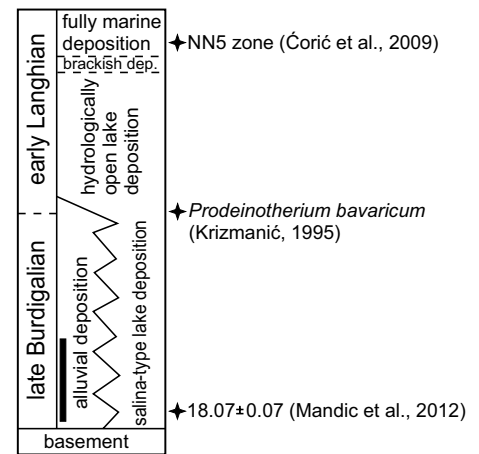


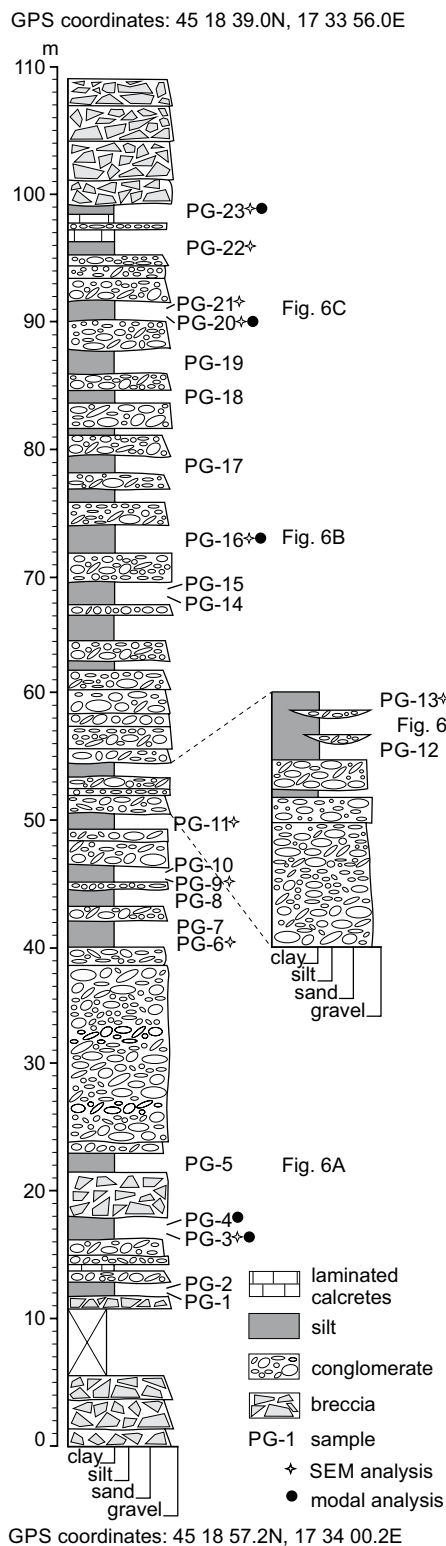
Figure 4. Compilation of early Miocene depositional environments in the North Croatian Basin (after Krizmanić, 1995; Čorić et al., 2009; Mandić et al., 2012). Asterisks show biostratigraphic and radiometric dating. The tentative stratigraphic position of the studied succession on Mount Požeška is represented by the black bar.

<4 μm , and a sandy silt sample PG-6, with a median size of 41 μm (Table 1). The sediments are poorly or very poorly sorted, with average value around 2.3 in all samples. Most of them have near-symmetrical grain-size distribution, but 10 samples display skewed distribution. In four samples, grain-size distribution is fine skewed; in four samples, it is coarse-skewed; and in two samples, it is strongly coarse-skewed (Table 1). All samples from BANSKO HILL in Baranja have very similar grain-size characteristics (Fig. 5B). They are very poorly sorted and contain 69%–76% silt-sized particles, 17%–22% clay-sized particles, and 3%–13% sand-sized particles. Their median grain size varies in the range of medium silt (16–32 μm), and skewness is strongly fine (Table 1). Comparison of samples from these two locations indicates that the silts from Mount Požeška contain more clay-sized particles and are generally finer than silts from BANSKO HILL.

Modal Analysis

There is a significant difference between the modal composition of samples PG-3 and PG-4 and the other four samples (PG-13, PG-16, PG-20 and PG-23; Fig. 5A). The composition of the LMF of samples PG-3 and PG-4 is characterized by the dominance of quartz, and rock fragments, while the other four samples, except for quartz and rock fragments, are rich in muscovite and contain fragments of volcanic glass. The HMF of all samples is rich in chlorites. Samples

A



B

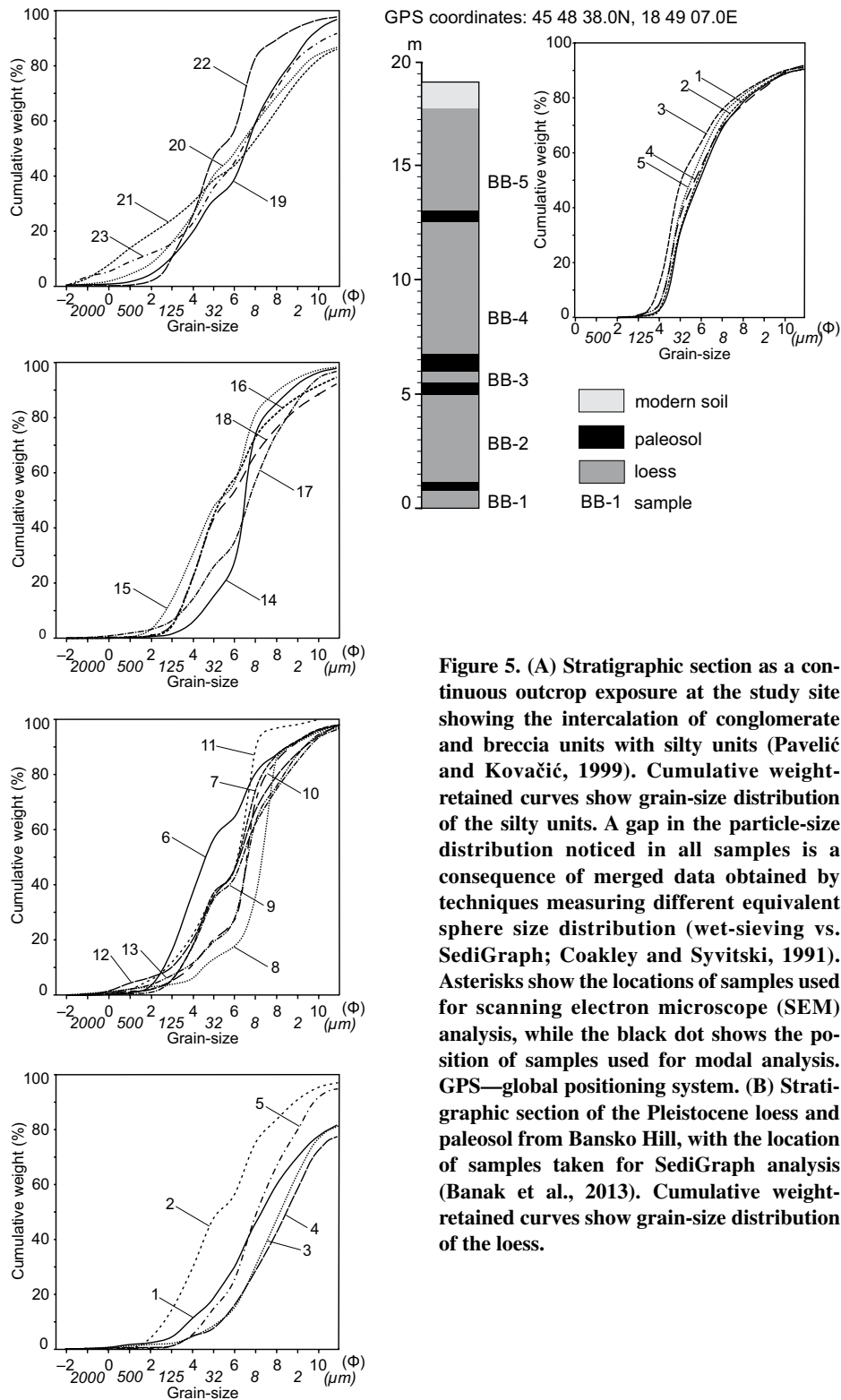


Figure 5. (A) Stratigraphic section as a continuous outcrop exposure at the study site showing the intercalation of conglomerate and breccia units with silty units (Pavelić and Kovačić, 1999). Cumulative weight-retained curves show grain-size distribution of the silty units. A gap in the particle-size distribution noticed in all samples is a consequence of merged data obtained by techniques measuring different equivalent sphere size distribution (wet-sieving vs. SediGraph; Coakley and Syvitski, 1991). Asterisks show the locations of samples used for scanning electron microscope (SEM) analysis, while the black dot shows the position of samples used for modal analysis. GPS—global positioning system. **(B)** Stratigraphic section of the Pleistocene loess and paleosol from Bansko Hill, with the location of samples taken for SediGraph analysis (Banak et al., 2013). Cumulative weight-retained curves show grain-size distribution of the loess.

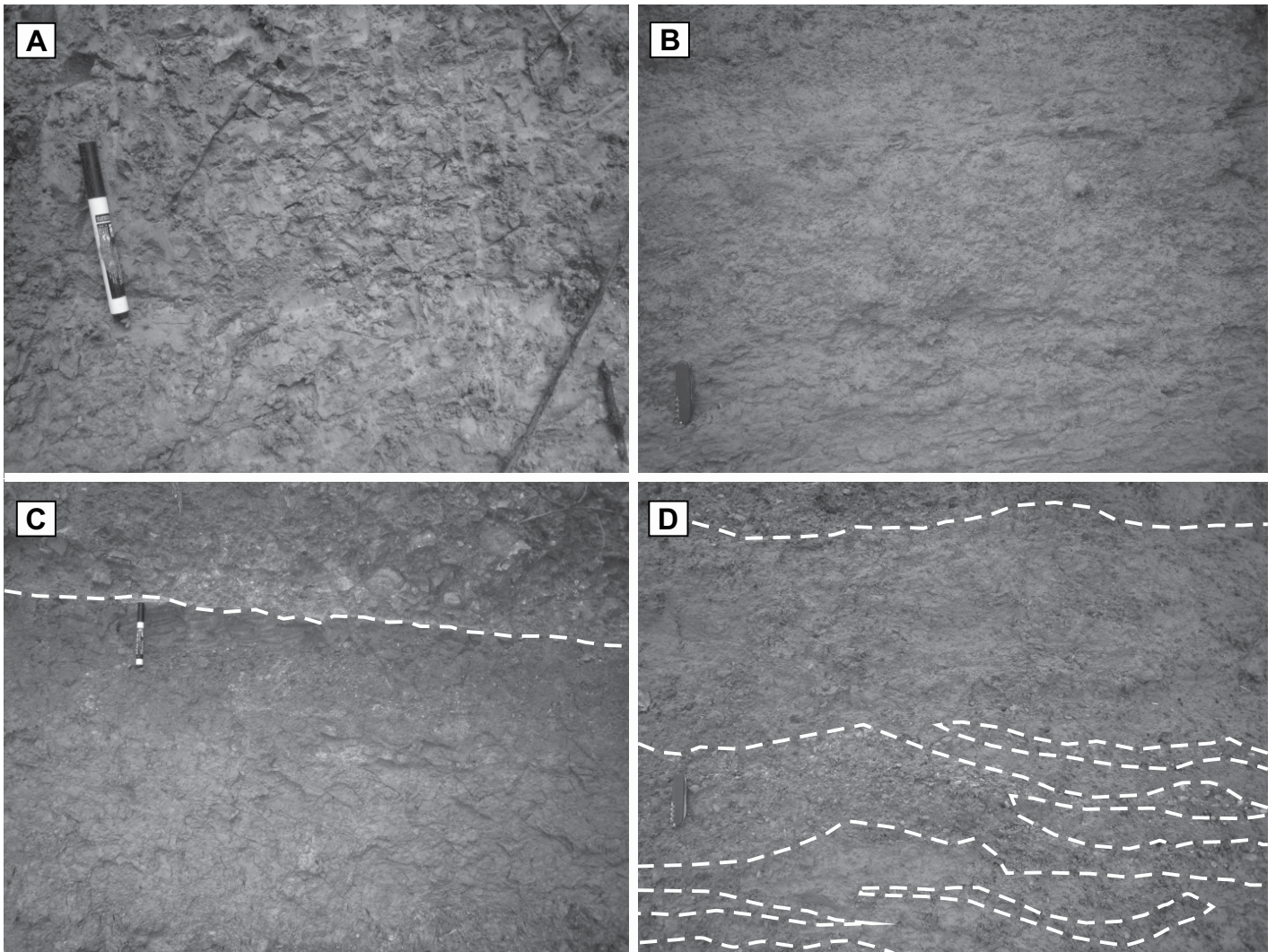


Figure 6. Photographs of structureless silty units characterized by yellowish to brownish colors. For the location of the photos in the section, see Figure 5A. (A) Structureless yellowish silt. Marker is 13 cm long. (B) Structureless brownish silt. Pocket knife is 9 cm long. (C) The red color of the upper part of the structureless brownish silt is a consequence of postdepositional pedogenic processes (at the level of the marker). The silt is overlain by conglomerates (upper part of the photo). Sharp boundary indicating erosion is marked by the dotted line. Marker is 13 cm long. (D) Structureless yellowish silt intercalated with conglomerate lenses. Key boundaries are marked by dotted lines. Pocket knife is 9 cm long.

PG-3 and PG-4 contain significant amounts of amphiboles. The other four samples are rich in epidote group minerals, garnets, and zircons, and also contain biotite.

SEM Analysis

Most quartz grains are blocky and of low relief, and more than 75% of the grains show low sphericity. Angular grains of sharp edges prevail, accounting for >70% of the total number of grains (Fig. 7). About 10% of grains are very angular or subrounded. Almost all grains have fracture faces on their surfaces, including conchoidal fractures and V-shaped percussion

marks. Conchoidal fractures were detected in >40% of the grains, with sizes mostly varying between a quarter and a fifth of the grains. V-shaped percussion marks of random orientation are visible in 10% of grains. The length of the microtextures varies between 2 and 9 μm . They are usually clustered on the smooth, flat surfaces of the grains. They are present in the form of individual microtextures in a smaller number. About 10% of grains have linear steps on the surface. Fewer than 5% of grains display conchoidal crushing features on their surfaces. Two big, straight grooves were detected on the surface of one grain in sample PG-20 (Fig. 7).

Palynological Analysis

Palynological analysis on nine samples coming from the fine-grained deposits yielded negative results. Very little, if any, organic material was obtained after mineral digestion with HCL and HF.

DISCUSSION

Eolian versus Fluvial Deposition

Fine-grained sedimentation is usually generated by particle decantation after suspension by weak currents in alluvial-fan environments such

TABLE 1. GRAIN-SIZE DISTRIBUTION AND COEFFICIENTS OF SAMPLES FROM FINE-GRAINED UNITS OF STUDIED SECTION ON MOUNT POŽEŠKA (PG) AND THE BANSKO HILL (BB)

Sample	Grain-size distribution (%)				Grain-size coefficients			
	Clay	Silt	Sand	Gravel	Median size (µm)	Mean size (µm)	Sorting	Sk
PG-1	40.24	48.40	11.32	0.04	6.49	6.00	2.57	-0.02
PG-2	16.24	54.24	29.48	0.04	26.23	22.93	2.41	0.15
PG-3	50.78	44.13	4.66	0.43	3.87	3.74	2.01	-0.08
PG-4	57.35	37.76	4.85	0.04	2.91	3.26	2.12	-0.21
PG-5	33.86	60.36	5.78	0.00	7.50	7.07	2.04	0.04
PG-6	12.58	49.52	37.80	0.10	40.68	30.77	2.27	0.30
PG-7	12.90	68.45	18.51	0.14	14.36	17.01	2.02	-0.08
PG-8	13.90	79.63	5.72	0.74	6.56	8.28	1.56	-0.32
PG-9	25.09	56.59	18.23	0.09	12.32	12.37	2.38	0.02
PG-10	14.88	73.70	10.90	0.52	11.08	12.74	1.88	-0.12
PG-11	2.98	74.59	22.29	0.14	15.01	23.26	1.77	-0.49
PG-12	20.44	58.92	20.44	0.20	13.89	14.90	2.59	-0.09
PG-13	24.01	64.17	11.32	0.50	10.28	10.33	2.20	-0.06
PG-14	14.8	79.03	6.13	0.04	11.41	11.46	1.61	0.04
PG-15	10.63	58.40	30.90	0.07	26.48	26.71	2.13	0.06
PG-16	18.40	59.06	22.51	0.03	24.11	18.09	2.30	0.30
PG-17	25.83	59.64	14.09	0.44	9.91	10.89	2.32	-0.09
PG-18	23.80	53.55	22.43	0.22	19.93	14.45	2.51	0.28
PG-19	26.03	54.10	19.37	0.50	11.00	12.49	2.54	-0.10
PG-20	30.69	42.99	25.59	0.73	14.58	12.51	3.14	0.03
PG-21	33.51	35.74	27.89	2.83	10.28	15.48	3.86	-0.24
PG-22	9.95	64.11	25.80	0.14	25.92	26.47	1.95	0.06
PG-23	26.90	49.96	19.73	3.41	12.61	14.01	3.12	-0.14
BB-1	21.54	74.95	3.51	0.00	16.91	11.72	2.11	0.39
BB-2	20.53	76.14	3.33	0.00	17.92	12.40	2.07	0.41
BB-3	17.88	69.40	12.72	0.00	30.26	17.43	2.16	0.54
BB-4	22.22	72.01	5.77	0.00	19.47	12.63	2.17	0.43
BB-5	18.77	76.09	5.14	0.00	21.65	14.43	2.04	0.47

as floodplains or abandoned channels (Miall, 1977). The silty units studied here were previously interpreted in such a way, in the context of an alluvial-fan environment (Pavelić and Kovačić, 1999). Characteristic depositional structures of floodplain deposits are well known, including plane-parallel lamination overlain by climbing ripple lamination and grading within thin beds from sand to clay (Allen, 1965). However, such structures were not observed in the studied sediments. Structureless silts and muds may occur in alluvial-fan environments, especially within gravelly and sandy braided streams, where they represent deposits from standing pools of water during low-stage channel abandonment. In such cases, the fine-grained deposits are usually only up to few centimeters thick and show plant root marks and desiccation cracks (Miall, 1978). However, the thickness of the silty units is up to 180 cm, and there is a lack of root marks and desiccation cracks. These features are not consistent with deposition in an alluvial-fan environment. Deposition by flowing water is not supported by SEM analysis of microtextures either. This analysis shows blocky silt-sized quartz grains with sharp edges, angular morphology, low-relief, conchoidal fractures, and rare occurrence of V-shaped percussion marks without preferred orientation, which are common characteristics of eolian dust- and sand-sized particles (Manker and Ponder, 1978; Whalley et al., 1982; Mahaney and Andres, 1996; Pye and Sperling, 1983; Wright, 2007).

The silty units are thus interpreted as having been deposited by wind. The lack of abrasion also indicates that grains did not experience previous fluvial transportation and diagenetic history, i.e., the grains were not deflated from a river floodplain, and are the result of the first cycle of a relatively short transport and deposition mechanism, although river floodplains can be an important source of loess (e.g., Stevens et al., 2013b; Nie et al., 2014). Such eolian deposits, which are predominantly composed of silt-sized particles and are characterized by the lack of any type of internal structures, are brownish yellow to yellow brownish color, and show evidence of postdepositional pedogenetic processes, as indicated by the red color and calcretes, may be considered as desert-type loess (cf. Tsoar and Pye, 1987; Pye, 1995; Smalley, 1995; Wright, 2001; Smith et al., 2002; Muhs, 2007; Smalley et al., 2011). Isolated grains up to 5 mm in diameter in the silt units are interpreted as having been deposited as rolling and rock-fall clasts from a nearby steep footwall block, as indicated by thick rock-fall breccia units in the succession, while sand-sized particles are probably a result of deposition by rolling and saltation.

Source of the Dust

The early Miocene deposition, characterized by alternation of alluvial and eolian phases, reflects the alternation of humid and arid cli-

mates (Pavelić and Kovačić, 1999; Ščavničar et al., 1983). The occurrence of the penecontemporaneous salina-type lake nearby additionally supports aridity in the area. In such climatic conditions, salina-type lake flats can produce silt-sized particles by salt weathering. This process is generated by the crystallization of salt, producing disintegration of rocks and sediments in hot deserts by size reduction and changes in the shape of surficial sediment clasts, which in turn produce conchoidal and blocky microtextures (Goudie and Cooke, 1970; Pye and Sperling, 1983; Pye, 1995; Smalley, 1995; Smith et al., 2002; Wright, 2007). Salt weathering could have occurred north of the study area, where a penecontemporaneous salina-type lake existed (Fig. 3). It was a relatively shallow and closed salt lake supplied by fluvial siliciclastic material derived from nearby uplifting blocks (Ščavničar et al., 1983). Evaporation of lake water probably generated salt crystallization and weathering of loose granular material on the dried-out lake flats in periods of high aridity, which produced a significant quantity of silt-sized particles (e.g., Pye and Sperling, 1983).

Additionally, desiccated lacustrine sediments could also act as a potential dust source, (e.g., Talbot et al., 1994; Nie et al., 2014), as indicated by the modal composition of the eolian silt represented by quartz, muscovite, volcanic glass, chlorite, amphiboles, garnets, and biotite, which strongly reflect the modal composition of salina-type lake deposits (Ščavničar et al., 1983). Minor differences in composition of the eolian silt from the lower, middle, and upper parts of the section are possible and could result from variations in the material transported by the rivers into the lake due to changes in the source area as the result of synrift tectonics. The lake was probably deflated under the influence of generally northerly winds, possibly blowing from the Central Paratethys Sea (Fig. 2), and eolian dust composed of silt- and clay-sized particles, and some sand-sized grains, was transported southward. There, a tectonically uplifting footwall block represented an obstacle to the northerly winds, causing the dust sedimentation that blanketed the alluvial deposits. This is supported by the grain microtextures, which indicate relatively short transport distances and a nearby source. This interpretation is in accordance with the suggestion of Pye and Sperling (1983), who proposed that a particularly favorable environment for silt formation might be expected to be where alluvial fans extend down from actively uplifting mountain fronts toward salina-lake basins.

Typically for loess, the silt-sized fraction is the dominant fraction in fine-grained early Miocene sediments from Mount Požeška (Table 1;

Figure 7. Scanning electron microscope (SEM) images of quartz grains showing microtextures. For sample locations, see Figure 5A. (A) Subangular grain with conchoidal fractures (1) and fracture faces (3) (sample PG-23). (B) Grain with conchoidal fractures (1) and fracture faces (3) (sample PG-23). (C) Subangular grain with conchoidal fractures (1), fracture faces (3), and linear steps (5) (sample PG-23). (D) Angular grain with conchoidal fractures (1), fracture faces (3), and linear steps (5) (sample PG-22). (E) Subangular grain with conchoidal fractures (1) and fracture faces (3) (sample PG-21). (F) Subangular grain with V-shaped percussion marks (2) and fracture faces (3) (sample PG-20). (G) Same grain with close-up of V-shaped percussion marks (2) (sample PG-20). (H) Subangular grain with conchoidal fractures (1), V-shaped percussion marks (2), and two straight grooves (6) (sample PG-20). (I) Grain with conchoidal fractures (1), V-shaped percussion marks (2), and conchoidal crushing features (4) (sample PG-20). (J) Grain with zoomed V-shaped percussion marks (2) (sample PG-21).

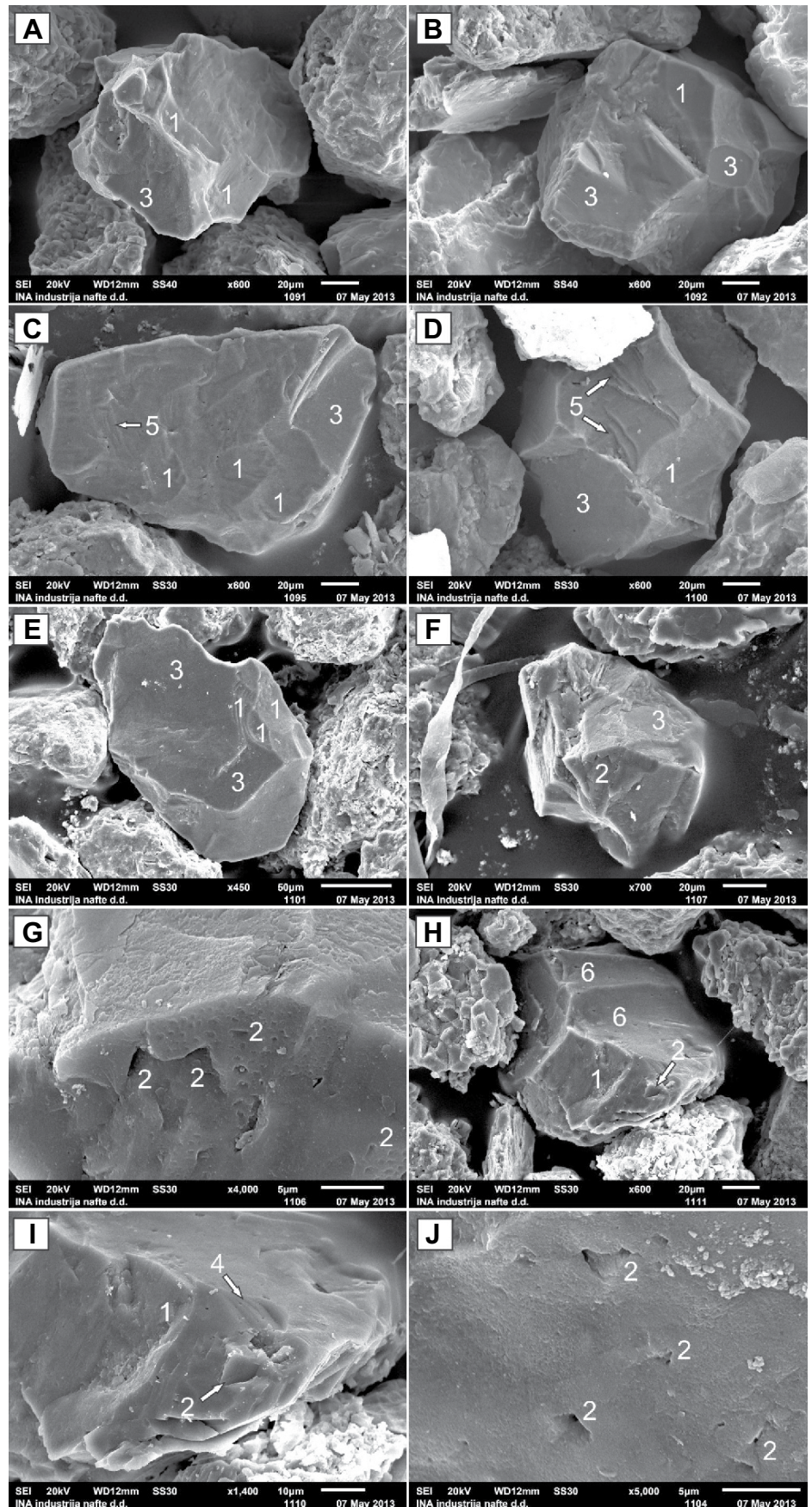


Fig. 5A). However, in comparing them with Pleistocene loess on the Bansko Hill, it is obvious that early Miocene loess contains more clay-sized particles; its median grain size (Md) is slightly smaller; and it is poorly sorted (Figs. 5A and 5B). The grain-size difference between the Pleistocene loess on Bansko Hill and early Miocene loess on Mount Požeška is probably a consequence of their different sources. The Pleistocene silt material was produced by multi-phase transport and depositional mechanisms preceding final deposition, which included initial glacial grinding, abrasion and freeze-thaw processes, fluvial transport, sedimentation in plains, dried sediment deflation, and eolian silt sedimentation (Banak et al., 2013). In contrast, deposition of the early Miocene loess was probably a result of deflation of silt-sized particles produced by salt weathering of loose granular material and desiccated lacustrine sediments on the dried-out lake mud flats, representing the first cycle of deposition. Those mud flats might represent the source of the clay-sized particles that are more abundant in the early Miocene loess than in the Pleistocene loess. Additionally, the larger proportion of clay-sized particles in the early Miocene loess could reflect deposition by a lower wind strength compared with the Pleistocene wind strength.

Similar early Miocene eolian deposits have not been discovered elsewhere in the North

Croatian Basin, and so these deposits represent the only known Miocene loess outside China (e.g., Guo et al., 2002; Garzzone et al., 2005).

Climatic Controls on Deposition

There is a general agreement among scientists that the late early Miocene was a time of relatively high global temperatures that culminated in the Miocene climatic optimum (Zachos et al., 2001). However, less is known about precipitation for the same time period. Our work suggests that the studied region was characterized by cyclic humidity changes, with periods of pronounced aridity in the late early Miocene. This is indicated by loess deposition and the occurrence of a salina-type lake generated under arid climates. The occurrence of loess units up to 180 cm thick indicates relatively long arid periods, but thin conglomerate lenses in the units reflect occasional rain events capable of activating the coarse fan material. High-energy alluvial mechanisms that transported coarse-grained material probably eroded the upper part of the loess layers, yielding the sharp contacts observed in the field (Fig. 5C). This suggests that arid periods of eolian dust deposition were probably longer than that indicated by the preserved thickness of the loess layers.

This study shows that at certain times, climate in the area was mostly semiarid, and this agrees with a previous study that also pointed to arid-

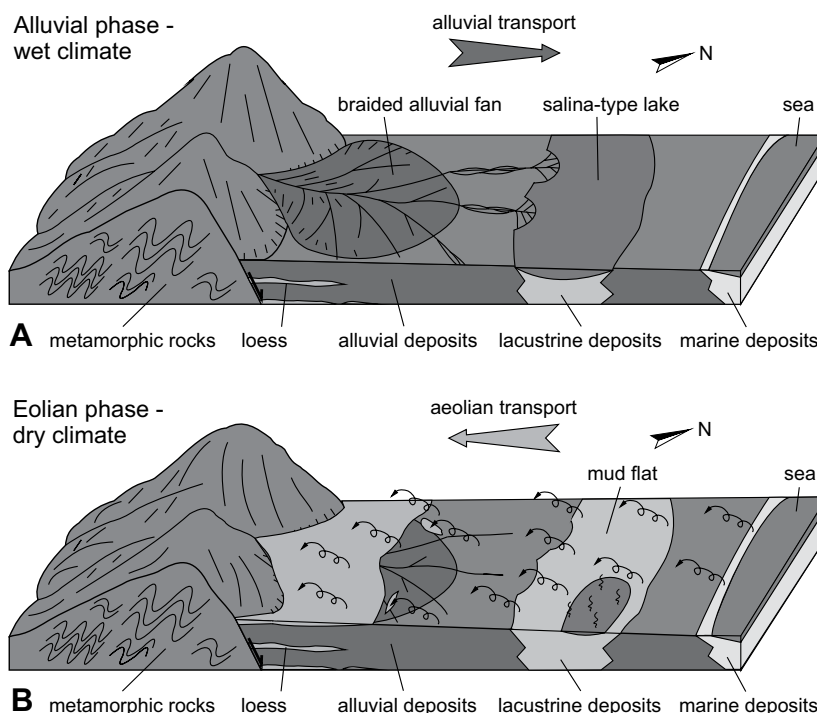
ity as the main control on the salina-type lake evolution (Ščavničar et al., 1983). Other early Miocene climate studies following different methodological approaches, such as palynology, paleobotany, sedimentology, and paleosol analysis, carried out in Central Europe show that the climate was subtropical with a strong seasonality in precipitation (Utescher et al., 2007; Jiménez-Moreno et al., 2009). The arid season seemed to be particularly important in shaping the environments in our area of study. This is because orbital changes control climate seasonality and therefore cyclic variations in the length of the dry season (Berger et al., 2006). Early Miocene aridity has been documented from freshwater lacustrine deposits in the Croatian part of the Adriatic coast (Pag and Sinj Basins; Fig. 1). This is indicated by the abundance of xeric indicators, such as *Olea* or the evergreen *Quercus*, in the pollen records from this area (Jiménez-Moreno et al., 2008, 2009). Aridity in the early Miocene is also interpreted from a paleobotanical study from Serbia that identified a xerothermic and evergreen flora (Utescher et al., 2007). The dry climate exerted controls on the loess and salina deposition despite, this occurring on a large island surrounded by seas (a potential source of higher humidity) in a mid-latitude paleogeographic location (Fig. 2).

The generally arid climate was frequently interrupted by relatively humid intervals that caused alluvial deposition (i.e., gravels) and deepening of the salina-lake, expanding its

water surface (Ščavničar et al., 1983), and ending loess deposition. The 109-m-thick succession indicates a long period of alternation of loess and alluvial deposition reflecting frequent alternation of arid and more humid phases in the late early Miocene (Fig. 8). The alluvial phase reflects deposition on the alluvial fan, and the transport of the material toward the salina-type lake (Fig. 8A), while the eolian phase was characterized by wind blowing toward the alluvial fan, which deflated the extending lake mud flat. Such loess-gravel interbedding can be compared to the Oligocene–early Miocene sequences of interbedded loess and soil units with orbital-scale cyclicity in China, where loess units indicate deposition in an arid interval while the soil reflects more humid intervals (Guo et al., 2002). However, the soil units on Mount Požeška are not well developed, probably due to erosion by water during humid periods.

This study agrees with other regional and European-scale paleoclimate studies that show climate cyclicity in precipitation, with a prominent, sustained dry cycle, and orbital-scale climate variability controlling paleoenvironmental and sedimentary changes in the area during the early Miocene. For example, in the nearby Sinj and Pag Basins, the late early Miocene environments and sedimentation were controlled by a climate characterized by cyclical alternations of generally arid and more humid phases (Jiménez-Moreno et al., 2008, 2009; Mandić et al., 2009). This is indicated by the alterna-

Figure 8. Depositional model for the alternation of alluvial and eolian phases in the area of northern Mount Požeška during the late early Miocene. (A) The alluvial phase was characterized by erosion of metamorphic rocks and deposition of the resulting fragments in the alluvial fan developed on the transition from slopes of uplifted footwall block to the hanging-wall valley. The transport of the material was generally northward, i.e., toward the salina-type lake. This phase was controlled by a wet climate. (B) During the eolian phase, the wind blowing toward the south deflated the wide mud flat developed due to the lake surface shrinking generated by a dry climate. The footwall block slopes acted as an obstacle to the northerly wind, causing deposition of dust together with sand-sized particles.



tion of xeric (i.e., *Olea*, evergreen *Quercus*) and hygrophilous (i.e., *Taxodium*-type, *Engelhardtia*) plant taxa that covaried with sedimentary changes indicating environmental changes (i.e., lake-level variations in both basins). The arid-humid cyclicity observed in the Pag Basin was interpreted as having been forced by 100 k.y. eccentricity cycles (Jiménez-Moreno et al., 2009). In another pollen study from an early Miocene lacustrine sedimentary sequence in NE Spain (Rubiños de Mora Basin), the humid and arid cycles seem to be caused by ~41 k.y. obliquity cycles (Jiménez-Moreno et al., 2007). The lack of a detailed chronological constraint prevented assignment of a definite periodicity to the loess/gravel sedimentary cycles documented here.

The observed eolian/alluvial sedimentary cycles terminated when a hydrologically open lake formed in the area around the end of the Burdigalian (ca. 16 Ma). This indicates that the climate changed toward a more humid one, as was previously indicated by a rich terrestrial paleofloristic assemblage from the area including *Phragmites oeningensis*, *Andromeda protozea*, *Myrica lignitum*, *Myrica hakeaefolia*, *Laurus primigenia*, *Cinnamomum* sp., and *Cassia* cf. *sagoriana* (Jamičić et al., 1987; Jungwirth and Đerek, 2000; Pavelić, 2001; Ćorić et al., 2009).

CONCLUSION

In this study, we suggest that silty units intercalated with conglomerates and breccia from a Lower Miocene terrestrial succession from the North Croatian Basin, previously interpreted as floodplain deposits of an alluvial fan, more likely represent loess or loess-like sediments. Most of the silt-sized particles were probably produced by salt-weathering processes on a salina-type lake flat during arid periods that existed penecontemporaneously with the alluvial fan. The particles were deflated together with clay-sized and some sand-sized particles by generally northerly winds and settled over coarse-grained material of the alluvial fan. The alluvial fan extended down from a tectonically uplifting footwall block that represented an obstacle to the northerly winds, causing deposition of the dust. The alluvial deposition was controlled by a more humid climate, so the intercalation of eolian silty units with alluvial conglomerates and breccias reflects cyclical alternation of arid and more humid periods in the early Miocene. This agrees with regional paleoclimate studies that show orbital-scale climate variability controlling paleoenvironmental and sedimentary changes in the area during the early Miocene.

ACKNOWLEDGMENTS

This paper was supported by projects no. 195-1951293-2703, 119-1191155-1159, and 181-181-1096-1093 of the Croatian Ministry of Science, Education and Sports, and by the University of Zagreb. Hans de Bruijn (Utrecht) is greatly acknowledged for providing information on the lack of micromammalian fossils in silty units, and Oleg Mandić (Vienna) is thanked for useful discussion. Hereby, we express our thanks to Tamara Troskot-Čorbić (Zagreb) and Renata Slavković (Zagreb) for providing technical support for producing images of quartz grains. The review of an early version of the manuscript by Zhengtang Guo (Beijing) and Thomas Stevens (Uppsala) is gratefully acknowledged. We would like to thank *GSA Bulletin* Editor Christian Koerber, Associate Editor Jeff Clark, Gabor Újvári, and an anonymous reviewer for their helpful comments.

REFERENCES CITED

- Allen, J.R.L., 1965, A review of the origin and characteristics of recent alluvial sediments: *Sedimentology*, v. 5, p. 89–191, doi:10.1111/j.1365-3091.1965.tb01561.x.
- Alonso-Zarza, A.M., Zhao, Z., Song, C.H., Li, J.J., Zhang, J., Martín-Perez, A., Martín-García, R., Wang, X.X., Zhang, Y., and Zhang, M.H., 2009, Mudflat/distal fan and shallow lake sedimentation (upper Vallesian-Turolian) in the Tianshui Basin, Central China: Evidence against the late Miocene eolian loess: *Sedimentary Geology*, v. 222, p. 42–51, doi:10.1016/j.sedgeo.2009.03.010.
- Banak, A., Mandić, O., Kovačić, M., and Pavelić, D., 2012, Late Pleistocene climate history of the Baranja loess plateau—Evidence from the Zmajevac loess-paleosol section (northeastern Croatia): *Geologia Croatica*, v. 65, p. 411–422.
- Banak, A., Pavelić, D., Kovačić, M., and Mandić, O., 2013, Sedimentary characteristics and source of late Pleistocene loess in Baranja (eastern Croatia): *Aeolian Research*, v. 11, p. 129–139, doi:10.1016/j.aeolia.2013.08.002.
- Berger, A., Loutre, M.F., and Mélice, J.L., 2006, Equatorial insolation: From precession harmonics to eccentricity frequencies: *Climate of the Past Discussion*, v. 2, p. 519–533, doi:10.5194/cpd-2-519-2006.
- Blott, S.J., and Pye, K., 2001, GRADISTAT: A grain size distribution and statistics package for the analysis of unconsolidated sediments: *Earth Surface Processes and Landforms*, v. 26, p. 1237–1248, doi:10.1002/esp.261.
- Coakley, J.P., and Syvitski, J.P.M., 1991, *SediGraph* technique, in Syvitski, J.P.M., ed., *Principles, Methods and Application of Particle Size Analysis*: New York, Cambridge University Press, p. 129–142.
- Ćorić, S., Pavelić, D., Rögl, F., Mandić, O., Vrabac, S., Avanić, R., and Vranjković, A., 2009, Revised middle Miocene datum for initial marine flooding of North Croatian Basins (Pannonian Basin system, Central Paratethys): *Geologia Croatica*, v. 62, p. 31–43.
- Faegri, K., and Iversen, J., 1989, *Textbook of Pollen Analysis*: New York, John Wiley & Sons, 328 p.
- Galović, L., Frechen, M., Halamić, J., Durn, G., and Romić, M., 2009, Loess chronostratigraphy in eastern Croatia—A luminescence dating approach: *Quaternary International*, v. 198, p. 85–97, doi:10.1016/j.quaint.2008.02.004.
- Garzzone, C.N., Ikari, M.J., and Basu, A.R., 2005, Source of Oligocene to Pliocene sedimentary rocks in the Linxia Basin in northeastern Tibet from Nd isotopes: Implications for tectonic forcing of climate: *Geological Society of America Bulletin*, v. 117, p. 1156–1166, doi:10.1130/B25743.1.
- Goddard, E.N., Trask, P., De Ford, R.K., Rove, O.N., Singewald, J.T., Jr., and Oberbach, R.M., 1963, Rock-Color Chart: New York, Geological Society of America, 4 p.
- Goudie, A., and Cooke, R., 1970, Experimental investigation of rock weathering by salts: *Area*, v. 4, p. 42–48.
- Guo, Z., Ge, J., Xiao, G., Hao, Q., Wu, H., Zhan, T., Liu, L., Qin, L., Zeng, F., and Yuan, B., 2010, Comment on “Mudflat/distal fan and shallow lake sedimentation (upper Vallesian-Turolian) in the Tianshui Basin, Central China: Evidence against the late Miocene eolian loess”: *Sedimentary Geology*, v. 230, p. 86–89, doi:10.1016/j.sedgeo.2010.06.019.
- Guo, Z.T., Ruddiman, W.F., Hao, Q.Z., Wu, H.B., Qiao, Y.S., Zhu, R.X., Peng, S.Z., Wei, J.J., Yuan, B.Y., and Liu, T.S., 2002, Onset of Asian desertification by 22 Myr ago inferred from loess deposits in China: *Nature*, v. 416, p. 159–163, doi:10.1038/416159a.
- Haase, D., Fink, J., Haase, G., Ruske, R., Pessi, M., Richter, H., Altermann, M., and Jaeger, K.-D., 2007, Loess in Europe—Its spatial distribution based on a European loess map, scale 1:2,500,000: *Quaternary Science Reviews*, v. 26, p. 1301–1312.
- Hajek-Tadesse, V., Belak, M., Sremac, J., Vrsaljko, D., and Wacha, L., 2009, Early Miocene ostracods from Sadovi section (Mt Požeška gora, Croatia): *Geologica Carpathica*, v. 60, p. 251–262, doi:10.2478/v10096-009-0017-0.
- Harzhauser, M., and Piller, W.E., 2007, Benchmark data of a changing sea—Palaeogeography, palaeobiogeography and events in the Central Paratethys during the Miocene: *Palaeogeography, Palaeoclimatology, Palaeoecology*, v. 253, p. 8–31, doi:10.1016/j.palaeo.2007.03.031.
- Hrvatski Geološki Institut (HGI), 2009, *Geološka Karta Republike Hrvatske: Hrvatski Geološki Institut, Zavod za Geologiju, Zagreb, scale 1:300,000.*
- Jamičić, D., Brkić, M., Crnko, J., and Vragović, M., 1987, *Osnovna Geološka Karta SFRJ 1:1000000. Tumač za list Orahovica L 33–96: Beograd, Geološki zavod, Zagreb, Savezni geološki zavod, Beograd, 72 p.*
- Jiménez-Moreno, G., Rodríguez-Tovar, F.-J., Pardo-Igúzquiza, E., Fauquette, S., Suc, J.-P., and Müller, P., 2005, High-resolution palynological analysis in late early-middle Miocene core from the Pannonian Basin, Hungary: Climatic changes, astronomical forcing and eustatic fluctuations in the Central Paratethys: *Palaeogeography, Palaeoclimatology, Palaeoecology*, v. 216, p. 73–97, doi:10.1016/j.palaeo.2004.10.007.
- Jiménez-Moreno, G., Abdul-Aziz, H., Rodríguez-Tovar, F.J., Pardo-Igúzquiza, E., and Suc, J.-P., 2007, Palynological evidence for astronomical forcing in early-middle Miocene lacustrine deposits from Rubielos de Mora Basin (NE Spain): *Palaeogeography, Palaeoclimatology, Palaeoecology*, v. 252, p. 601–616, doi:10.1016/j.palaeo.2007.05.013.
- Jiménez-Moreno, G., Mandić, O., Harzhauser, M., Pavelić, D., and Vranjković, A., 2008, Vegetation and climate dynamics during the early middle Miocene from Lake Sinj (Dinaride Lake system, SE Croatia): *Review of Palaeobotany and Palynology*, v. 152, p. 237–245, doi:10.1016/j.revpalbo.2008.05.005.
- Jiménez-Moreno, G., de Leeuw, A., Mandić, O., Harzhauser, M., Pavelić, D., Krijgsman, W., and Vranjković, A., 2009, Integrated stratigraphy of the early Miocene lacustrine deposits of Pag Island (SW Croatia): *Palaeovegetation and environmental changes in the Dinaride Lake system: Palaeogeography, Palaeoclimatology, Palaeoecology*, v. 280, p. 193–206, doi:10.1016/j.palaeo.2009.05.018.
- Jungwirth, E., and Đerek, T., 2000, Osobitosti paleoflore lokaliteta Planina, in Vlahović, I., and Biondić, R., eds., *Proceedings Second Croatian Geological Congress, Cavtat–Dubrovnik, 17–20.05.2000: Zagreb, Croatia, Institute of Geology*, p. 225–229.
- Kovács, J., 2008, Grain-size analysis of the Neogene red clay formation in the Pannonian Basin: *International Journal of Earth Sciences*, v. 97, p. 171–178, doi:10.1007/s00531-006-0150-2.
- Kovács, J., Fábán, Sz.A., Varga, G., Újvári, G., Varga, Gy., and Dezső, J., 2011, Plio-Pleistocene red clay deposits in the Pannonian Basin: A review: *Quaternary International*, v. 240, p. 35–43, doi:10.1016/j.quaint.2010.12.013.
- Krizmanić, K., 1995, Palynology of the Miocene bentonite from Gornja Jelenska (Mount Moslavačka Gora, Croatia): *Geologia Croatica*, v. 48, p. 147–154.
- Kukla, G., 1987, Loess stratigraphy in central China: *Quaternary Science Reviews*, v. 6, p. 191–219, doi:10.1016/0277-3791(87)90004-7.

- Liu, X.M., Rolph, T., An, Z., and Hesse, P., 2003, Paleoclimatic significance of magnetic properties on the red clay underlying the loess and paleosols in China: Palaeogeography, Palaeoclimatology, Palaeoecology, v. 199, p. 153–166, doi:10.1016/S0031-0182(03)00504-2.
- Mahaney, W.C., and Andres, W., 1996, Scanning electron microscopy of quartz sand from the north-central Saharan Desert of Algeria: Zeitschrift für Geomorphologie N.F., v. 103, p. 179–192.
- Malvić, T., 2012, Review of Miocene shallow marine and lacustrine depositional environments in northern Croatia: Geological Quarterly, v. 56, p. 493–504, doi:10.7306/gq.1035.
- Mandić, O., Pavelić, D., Harzhauser, M., Zupanić, J., Reischenbacher, D., Sachsenhofer, R.F., Tadej, N., and Vranjković, A., 2009, Depositional history of the Miocene Lake Sinj (Dinaride Lake system, Croatia): The long-lived hard-water lake in a pull-apart tectonic setting: Journal of Paleolimnology, v. 41, p. 431–452, doi:10.1007/s10933-008-9235-1.
- Mandić, O., de Leeuw, A., Bulić, J., Kuiper, K.F., Krijgsmann, W., and Jurišić-Poljšak, Z., 2012, Paleogeographic evolution of the southern Pannonian Basin: $^{40}\text{Ar}/^{39}\text{Ar}$ age constraints on the Miocene continental series of northern Croatia: International Journal of Earth Sciences, v. 101, p. 1033–1046, doi:10.1007/s00531-011-0695-6.
- Mange, M.A., and Maurer, H.F.W., 1992, Heavy Minerals in Colour: London, Chapman and Hall, 151 p.
- Manker, J.P., and Ponder, R.D., 1978, Quartz grain surface features from fluvial environments of northeastern Georgia: Journal of Sedimentary Petrology, v. 48, p. 1227–1232.
- Márton, E., Pavelić, D., Tomljenović, B., Pamić, J., and Márton, P., 1999, First paleomagnetic results on Tertiary rocks from the Slavonian Mountains in the Southern Pannonian Basin, Croatia: Geologica Carpathica, v. 50, p. 273–279.
- Márton, E., Pavelić, D., Tomljenović, B., Avanić, R., Pamić, J., and Márton, P., 2002, In the wake of a counterclockwise rotating Adriatic microplate: Neogene paleomagnetic results from northern Croatia: International Journal of Earth Sciences, v. 91, p. 514–523, doi:10.1007/s00531-001-0249-4.
- Márton, E., Jelen, B., Tomljenović, B., Pavelić, D., Poljak, M., Márton, P., Avanić, R., and Pamić, J., 2006, Late Neogene counterclockwise rotation in the SW part of the Pannonian Basin: Geologica Carpathica, v. 57, p. 41–46.
- Miall, A.D., 1977, A review of the braided river depositional environments: Earth-Science Reviews, v. 13, p. 1–62, doi:10.1016/0012-8252(77)90055-1.
- Miall, A.D., 1978, Facies types and vertical profiles in braided river deposits: A summary, in Miall, A.D., ed., Fluvial Sedimentology: Canadian Society of Petroleum Geologists Memoir 5, p. 597–604.
- Muhs, D.R., 2007, Loess deposits, origins, and properties, in Elias, S., ed., The Encyclopedia of Quaternary Sciences: Amsterdam, Netherlands, Elsevier, p. 1405–1418.
- Muhs, D.R., 2013, The geologic records of dust in the Quaternary: Aeolian Research, v. 9, p. 3–48, doi:10.1016/j.aeolia.2012.08.001.
- Nie, J., Peng, W., Möller, A., Song, Y., Stockli, D.F., Stevens, T., Horton, B.K., Liu, S., Bird, A., Oalman, J., Gong, H., and Fang, X., 2014, Provenance of the Upper Miocene–Pliocene red clay deposits of the Chinese Loess Plateau: Earth and Planetary Science Letters, v. 407, p. 35–47, doi:10.1016/j.epsl.2014.09.026.
- Pavelić, D., 2001, Tectonostratigraphic model for the North Croatian and North Bosnian sector of the Miocene Pannonian Basin system: Basin Research, v. 13, p. 359–376, doi:10.1046/j.0950-091x.2001.00155.x.
- Pavelić, D., and Kovačić, M., 1999, Lower Miocene alluvial deposits of the Požeška Mount (Pannonian Basin, northern Croatia): Cycles, megacycles and tectonic implications: Geologia Croatica, v. 52, p. 67–76.
- Pavelić, D., Miknić, M.A., and Sarkotić Šlat, M., 1998, Early to middle Miocene facies succession in lacustrine and marine environments on the southwestern margin of the Pannonian Basin system (Croatia): Geologica Carpathica, v. 49, p. 433–443.
- Pavelić, D., Avanić, R., Bakrač, K., and Vrsaljko, D., 2001, Early Miocene braided river and lacustrine sedimentation in the Kalnik Mountain area (Pannonian Basin system, NW Croatia): Geologica Carpathica, v. 52, p. 375–386.
- Pye, K., 1995, The nature, origin and accumulation of loess: Quaternary Science Reviews, v. 14, p. 653–667, doi:10.1016/0277-3791(95)00047-X.
- Pye, K., and Sperling, H.B., 1983, Experimental investigation of silt formation by static breakage process: The effect of temperature, moisture and salt on quartz dune sand and granitic regolith: Sedimentology, v. 30, p. 49–62, doi:10.1111/j.1365-3091.1983.tb00649.x.
- Qiang, X.K., An, Z.S., Song, Y.G., Chang, H., Sun, Y.B., Liu, W.G., Ao, H., Dong, J.B., Fu, C.F., Wu, F., Lu, F.Y., Cai, Y.J., Zhou, W.J., Cao, J.J., Xu, X.W., and Ai, L., 2011, New eolian red clay sequence on the western Chinese Loess Plateau linked to onset of Asian desertification about 25 Ma ago: Science China–Earth Science, v. 54, p. 136–144.
- Royden, L.H., 1988, Late Cenozoic tectonics of the Pannonian Basin system, in Royden, L.H., and Horváth, F., eds., The Pannonian Basin. A Study in Basin Evolution: American Association of Petroleum Geologists Memoir 45, p. 27–48.
- Ščavničar, S., Krkalo, E., Ščavničar, B., Halle, R., and Tibljaš, D., 1983, Naslage s analimom u Poljanskoj: Zagreb, Rad Jugoslavenske Akademije Znanosti i Umjetnosti, v. 404, p. 137–169.
- Smalley, I., 1995, Making the material: The formation of silt-sized primary mineral particles for loess deposits: Quaternary Science Reviews, v. 14, p. 645–651, doi:10.1016/0277-3791(95)00046-1.
- Smalley, I., Marković, S.B., and Svirčev, Z., 2011, Loess is (almost totally formed by) the accumulation of dust: Quaternary International, v. 240, p. 4–11, doi:10.1016/j.quaint.2010.07.011.
- Smith, B.J., Wright, J.S., and Whalley, W.B., 2002, Sources of non-glacial, loess-size quartz silt and the origins of “desert loess”: Earth-Science Reviews, v. 59, p. 1–26, doi:10.1016/S0012-8252(02)00066-1.
- Stevens, T., Adamiec, G., Bird, A.F., and Lu, H., 2013a, An abrupt shift in dust source on the Chinese Loess Plateau revealed through high sampling resolution OSL dating: Quaternary Science Reviews, v. 82, p. 121–132, doi:10.1016/j.quascirev.2013.10.014.
- Stevens, T., Carter, A., Watson, T.P., Vermeesch, P., Andò, S., Bird, A.F., Lu, H., Garzanti, E., Cottam, M.A., and Sevastjanova, I., 2013b, Genetic linkage between the Yellow River, the Mu Us desert and the Chinese Loess Plateau: Quaternary Science Reviews, v. 78, p. 355–368, doi:10.1016/j.quascirev.2012.11.032.
- Sun, J., Ye, J., Wu, W., Ni, X., Bi, S., Zhang, Z., Liu, W., and Meng, J., 2010, Late Oligocene–Miocene mid-latitude aridification and wind patterns in the Asian interior: Geology, v. 38, p. 515–518, doi:10.1130/G30776.1.
- Talbot, M.R., Holm, K., and Williams, M.A.J., 1994, Sedimentation in low-gradient desert margin systems: A comparison of the Late Triassic of northwest Somerset (England) and the late Quaternary of east-central Australia, in Rosen, M.R., ed., Paleoclimate and Basin Evolution of Playa Systems: Geological Society of America Special Paper 289, p. 97–117.
- Tsoar, H., and Pye, K., 1987, Dust transport and the question of desert loess formation: Sedimentology, v. 34, p. 139–153, doi:10.1111/j.1365-3091.1987.tb00566.x.
- Utescher, T., Djordjević-Milutinović, D., Bruch, A., and Mosbrugger, V., 2007, Palaeoclimate and vegetation change in Serbia during the last 30 Ma: Palaeogeography, Palaeoclimatology, Palaeoecology, v. 253, p. 141–152, doi:10.1016/j.palaeo.2007.03.037.
- Van Hoesen, J.G., and Orndorff, R.L., 2004, A comparative SEM study assessing the micromorphology of glaciated clasts of varying lithologies: Canadian Journal of Earth Sciences, v. 41, p. 1123–1139, doi:10.1139/e04-056.
- von Leonhard, K.C., 1823–1824, Charakteristik der Fallsarten: Heidelberg, Engelmann, 3 volumes.
- Vos, K., Vendenbergh, N., and Elsen, J., 2014, Surface textural analysis of quartz grains by scanning electron microscopy (SEM): From sample preparation to environmental interpretation: Earth-Science Reviews, v. 128, p. 93–104, doi:10.1016/j.earscirev.2013.10.013.
- Wacha, L., Mikulčić Pavlaković, S., Novothny, Á., Crnjaković, M., and Frechen, M., 2011, Luminescence dating of Upper Pleistocene loess from the Island of Susak in Croatia: Quaternary International, v. 234, p. 50–61, doi:10.1016/j.quaint.2009.12.017.
- Whalley, W.B., Marshall, J.R., and Smith, B.J., 1982, Origin of desert loess from some experimental observations: Nature, v. 300, p. 433–435, doi:10.1038/300433a0.
- Wright, J.S., 2001, “Desert” loess versus “glacial” loess: Quartz silt formation, source areas and sediment pathways in the formation of loess deposits: Geomorphology, v. 36, p. 231–256, doi:10.1016/S0169-555X(00)00060-X.
- Wright, J.S., 2007, An overview of the role of weathering in the production of quartz silt: Sedimentary Geology, v. 202, p. 337–351, doi:10.1016/j.sedgeo.2007.03.024.
- Zachos, J., Pagani, M., Sloan, L., Thomas, E., and Billups, K., 2001, Trends, rhythms, and aberrations in global climate 65 Ma to present: Science, v. 292, p. 686–693, doi:10.1126/science.1059412.
- Zhan, T., Guo, Z., Wu, H., Ge, J., Zhou, X., Wu, C., and Zeng, F., 2010, Thick Miocene eolian deposits on the Huajialing Mountains: The geomorphic evolution of the western Loess Plateau: Science China–Earth Sciences, v. 54, p. 241–248.

SCIENCE EDITOR: CHRISTIAN KOEBERL
ASSOCIATE EDITOR: JEFFREY CLARK

MANUSCRIPT RECEIVED 21 JANUARY 2015
REVISED MANUSCRIPT RECEIVED 16 JUNE 2015
MANUSCRIPT ACCEPTED 8 JULY 2015

Printed in the USA